A Density Functional Study on Beryllium-Doped Carbon Dianion Clusters C_nBe^{2-} ($n = 4-14$)

M. D. Chen,* X. B. Li, J. Yang, and Q. E. Zhang

State Key Laboratory of Physical Chemistry of Solid Surface, Department of Chemistry, Center for Theoretical Chemistry, College of Chemistry and Chemical Engineering, Xiamen University, Xiamen 361005, People's Republic of China

C. T. Au

Department of Chemistry, Hong Kong Baptist University, Kowloon Tong, Hong Kong, People's Republic of China

Received: August 26, 2005; In Final Form: January 20, 2006

Making use of the software of molecular graphics, we designed numerous models of C_nBe^{2-} ($n = 4-14$). We carried out geometry optimization and calculation on vibration frequency by means of the B3LYP density functional method. After comparison of structure stability, we found that the ground-state isomers of C_nBe^{2-} ($n = 4-14$) are linear with the beryllium atom located inside the C_n chain. When a side carbon chain is with an even number of carbon atoms, it is polyacetylene-like, whereas when a side chain is with an odd number of carbon atoms, it is cumulene-like. The C_nBe^{2-} ($n = 4-14$) clusters with an even number of carbon atoms are more stable than that with an odd number of carbon atoms, matching the peak pattern observed in accelerator mass spectrometry (AMS) and Coulomb Explosion Imaging (CEI) investigations of C_nBe^{2-} ($n = 4-14$). The trend of such odd/even alternation is explained based on concepts of bonding characteristics, electronic configuration, electron detachment, and incremental binding energy.

1. Introduction

The discovery of carbon compounds and clusters of novelty have opened up research fields of new dimensions.[1,2] Carbon clusters doped with a heteroatom have attracted immense attention in recent years, and their ions are considered to have structures analogous to those of C_n. By means of secondary ionic emission or laser ionization, a series of hetero-carbon anionic C_nX^- clusters were generated by adding a heteroatom X into the corresponding C_n^- clusters, where X is either a main group, a transition, or a nonmetal element.[3−7] To explore the intriguing experimental observations, theoretical investigations on C_nX^- clusters such as C_nSe^-,[8] C_nN^-,[9,10] C_nB^-,[11] C_nP^-,[12−15] SiC_n^-,[16,17] C_nSe^-,[18] RbC_n^-,[19] C_nH^-,[20] PbC_n^-,[21] MgC_n^-,[22,23] CaC_n^-,[24] NaC_n^-,[25] AlC_n^-,[26,27] ClC_n^-,[28] and C_nAs^- [29] were conducted.

Turning to dianions, several small ones are of paramount importance in chemistry; the most prominent examples are CO_3^{2-} and SO_4^{2-}.[30] Compared to a hetero-carbon anion that is singly charged, the doubly charged one behaves very differently. Because of the strong Coulomb repulsion induced by the added electron, small dianions are unlikely to exist as stable gas-phase entities. There are only a small number of experimental and theoretical investigations on hetero-carbon dianion clusters. Klein et al. observed BeC_n^{2-} ($n = 4-14$) by accelerator mass spectrometry (AMS) and Coulomb Explosion Imaging (CEI).[31] Gnaser et al. produced SiC_n^{2-} ($n = 6, 8, 10$) [32] and OC_n^{2-} ($n = 5-19$) [33] in sputtering. Dreuw et al. carried out theoretical studies on $Si_xC_y^{2-}$ ($x = 1, 2$, $y = 4-9$),[34,35] OC_n^2 ($n = 5-8$),[33] and BeC_n^{2-} ($n = 4, 6$)[36] by means of standard ab initio methods. Shi et al. conducted ab initio calculation of the repulsive Coulomb barrier for several geometrically stable isomers of C_4Be^{2-} dianions.[37] Trindle et al. developed a set of small open shell stable dianions by means of ROMP2, CCSD, and DFT calculations.[38]

In the AMS figure of the relative intensity of C_nBe^{2-} ($n = 4-14$) anions,[31] the dianionic clusters show an extreme odd/even behavior: the dianions with even number of carbon atoms are more prominent. To explore the experimental observation theoretically, we designed structural models of C_nBe^{2-} ($n = 4-14$) and performed geometry optimization and calculations on vibration frequencies by means of the B3LYP density functional method. The geometry structure, stability, electronic configuration, bonding character, electron detachment, and incremental binding energy of the dianionic clusters were examined. Based on the results, we provide explanation on why the C_nBe^{2-} ($n = 4-14$) isomers with even n are more stable than those with odd n. The outcome can serve as a guideline for the synthesis of related materials as well as for future theoretical studies of carbon/beryllium binary clusters.

2. Computational Methods

During the investigation, devices for molecular graphics, molecular mechanics, and quantum chemistry were used. First, a three-dimensional model of a cluster was designed using HyperChem for Windows[39] on a PC/Pentium IV computer. Then, the model was optimized by MM+ molecular mechanics and semiempirical PM3 quantum chemistry. Last, geometry optimization and calculations of vibration frequencies were conducted using the B3LYP density functional method of the Gaussian 98 package[40] with 6-31G* basis sets, i.e., Becke's 3-parameter nonlocal exchange functional with the correlation functional of Lee−Yang−Parr.[41,42] The single-point energy calculations following the optimizations were performed using the larger 6-311+G* basis set (i.e., B3LYP/6-311+G*//B3LYP/6-31G*).[43] (It has been pointed out by Foresman et al. that

10.1021/jp054830g CCC: $33.50 © 2006 American Chemical Society
Published on Web 03/16/2006

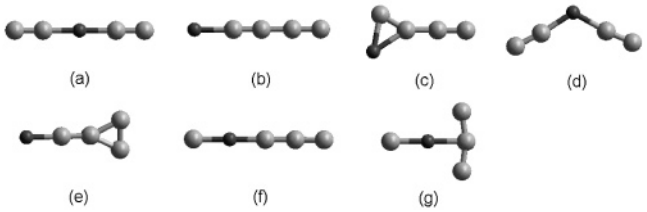

Figure 1. Seven isomers of C_4Be^{2-}.

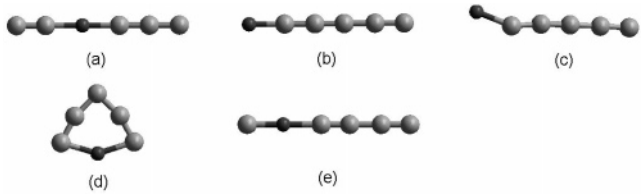

Figure 2. Five isomers of C_5Be^{2-}.

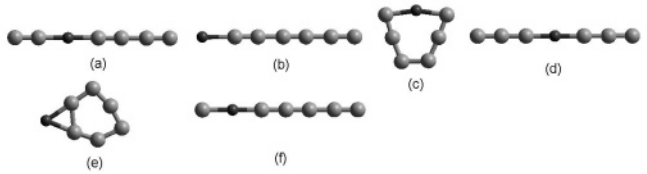

Figure 3. Six isomers of C_6Be^{2-}.

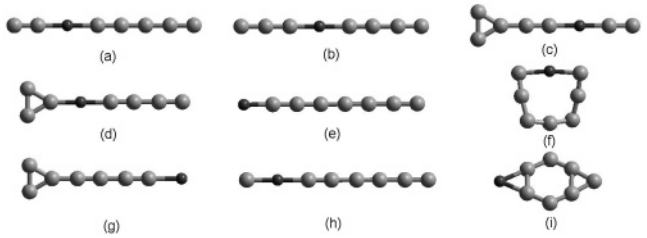

Figure 4. Nine isomers of C_7Be^{2-}.

geometries computed with more expensive basis sets do not necessarily lead to more accurate final results.[44]) Since the change of zero-point energy (ZPE) could only be affected slightly by the quality of the employed method,[36] all energies were calculated with ZPE correction at the B3LYP/6-31G* level. The optimized models were again displayed using HyperChem for Windows. The data of partial charges and bond orders were explored with Gaussian Natural Bond Orbital (NBO). All of the calculations were carried out on the servers of SGI.

3. Results and Discussion

3.1. Geometries and Energies. At the beginning of the study, nothing was known other than the C_nBe^{2-} ($n = 4-14$) formula. The assumption of a reasonable geometrical structure was the initial step for the optimization of the new dianions. We examined a huge number of isomers, among which are linear, cyclic, and bicyclic, as well as three-dimensional structures. In this paper, those with imaginary frequencies, higher energy, and large spin contamination are excluded. Shown in Figures 1−11 are the isomers corresponding to local minima of C_nBe^{2-} ($n = 4-14$) with real vibration frequencies. Most of the models depicted here have never been reported before. In each figure, the models are arranged in the order of ascending total energy; light gray (bigger) balls represent carbon atoms and dark gray (smaller) ones denote beryllium atoms.

Listed in Table 1 are the symmetries, electronic states, total energies, and relative energies of the C_nBe^{2-} ($n = 4-14$) structures. According to the relative energies, the ground-state

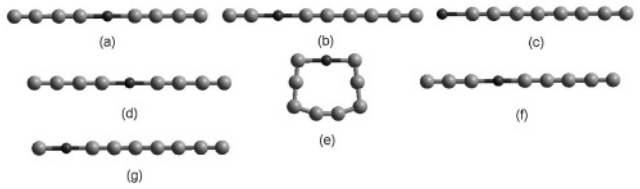

Figure 5. Seven isomers of C_8Be^{2-}.

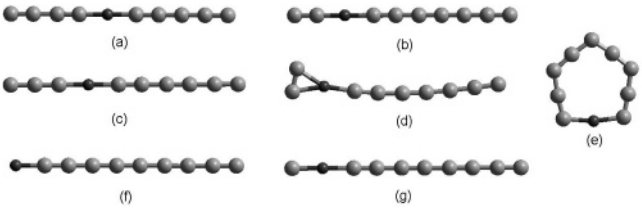

Figure 6. Seven isomers of C_9Be^{2-}.

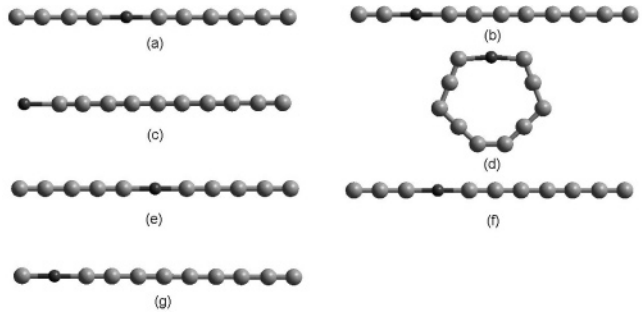

Figure 7. Seven isomers of $C_{10}Be^{2-}$.

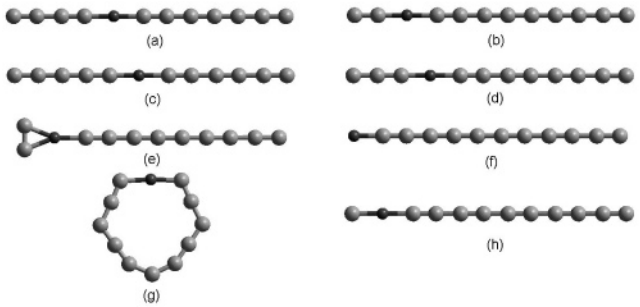

Figure 8. Eight isomers of $C_{11}Be^{2-}$.

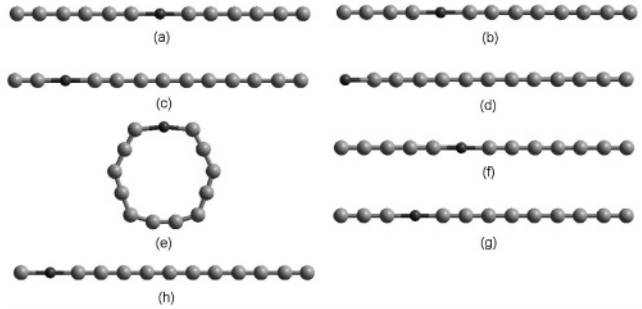

Figure 9. Eight isomers of $C_{12}Be^{2-}$.

geometries are linear configurations with the beryllium atom located at different positions inside the molecular chains. The most stable C_4Be^{2-}, C_8Be^{2-}, and $C_{12}Be^{2-}$ structures (models 1a, 5a, and 9a, respectively) are with the beryllium atom located at the center of the chain. For the most stable isomers of C_5Be^{2-}, C_6Be^{2-}, and C_7Be^{2-}, the beryllium atom is at the third position as viewed from the left of the chain (models 2a, 3a, and 4a, respectively). Models 6a, 7a, 8a, and 10a are respectively the structures of C_9Be^{2-}, $C_{10}Be^{2-}$, $C_{11}Be^{2-}$, and $C_{13}Be^{2-}$ with the

TABLE 1: Symmetries, Electronic States, Total Energies (au), and Relative Energies (kcal/mol) of C_nBe^{2-} ($n = 4-14$)

figure	cluster	symmetry	state	total energy	relative energy	figure	cluster	symmetry	state	total energy	relative energy
1a	C_4Be^{2-}	$D_{\infty h}$	$^1\Sigma_g$	−167.0026	0.00	7a	$C_{10}Be^{2-}$	$C_{\infty v}$	$^1\Sigma^+$	−395.6066	0.00
1b	C_4Be^{2-}	$C_{\infty v}$	$^1\Sigma^+$	−166.9712	19.75	7b	$C_{10}Be^{2-}$	$C_{\infty v}$	$^1\Sigma^+$	−395.5965	6.34
1c	C_4Be^{2-}	C_s	^{3}A	−166.9021	63.07	7c	$C_{10}Be^{2-}$	C_s	^{1}A	−395.5443	39.13
1d	C_4Be^{2-}	C_{2v}	$^3B_2$	−166.8907	70.24	7d	$C_{10}Be^{2-}$	C_{2v}	$^1A_1$	−395.5272	49.81
1e	C_4Be^{2-}	C_s	^{3}A	−166.8744	80.49	7e	$C_{10}Be^{2-}$	$D_{\infty h}$	$^1\Sigma_g$	−395.4969	68.87
1f	C_4Be^{2-}	$C_{\infty v}$	$^1\Sigma^+$	−166.8079	122.18	7f	$C_{10}Be^{2-}$	$C_{\infty v}$	$^1\Sigma^+$	−395.4910	72.54
1g	C_4Be^{2-}	C_{2v}	$^3B_2$	−166.7788	140.46	7g	$C_{10}Be^{2-}$	$C_{\infty v}$	$^1\Sigma^+$	−395.4166	119.23
2a	C_5Be^{2-}	$C_{\infty v}$	$^3\Sigma^-$	−205.0566	0.00	8a	$C_{11}Be^{2-}$	$C_{\infty v}$	$^3\Sigma^-$	−433.6682	0.00
2b	C_5Be^{2-}	$C_{\infty v}$	$^3\Sigma^-$	−205.0200	22.96	8b	$C_{11}Be^{2-}$	$C_{\infty v}$	$^3\Sigma^-$	−433.6625	3.54
2c	C_5Be^{2-}	C_s	^{1}A	−205.0067	31.34	8c	$C_{11}Be^{2-}$	$C_{\infty v}$	$^3\Sigma^-$	−433.6621	3.78
2d	C_5Be^{2-}	C_{2v}	$^1A_1$	−204.9986	36.41	8d	$C_{11}Be^{2-}$	$C_{\infty v}$	$^3\Sigma^-$	−433.6460	13.89
2e	C_5Be^{2-}	$C_{\infty v}$	$^3\Sigma^-$	−204.9700	54.37	8e	$C_{11}Be^{2-}$	C_s	^{1}A	−433.6363	19.99
3a	C_6Be^{2-}	$C_{\infty v}$	$^1\Sigma^+$	−243.2136	0.00	8f	$C_{11}Be^{2-}$	$C_{\infty v}$	$^3\Sigma^-$	−433.6288	24.70
3b	C_6Be^{2-}	$C_{\infty v}$	$^1\Sigma^+$	−243.1690	28.01	8g	$C_{11}Be^{2-}$	C_{2v}	$^3A_2$	−433.5980	44.06
3c	C_6Be^{2-}	C_s	^{1}A	−243.1092	65.53	8h	$C_{11}Be^{2-}$	$C_{\infty v}$	$^3\Sigma^-$	−433.5687	62.40
3d	C_6Be^{2-}	$D_{\infty h}$	$^1\Sigma_g$	−243.0846	80.92	9a	$C_{12}Be^{2-}$	$D_{\infty h}$	$^1\Sigma_g$	−471.7932	0.00
3e	C_6Be^{2-}	C_s	^{1}A	−243.0571	98.21	9b	$C_{12}Be^{2-}$	$C_{\infty v}$	$^1\Sigma^+$	−471.7910	1.34
3f	C_6Be^{2-}	$C_{\infty v}$	$^1\Sigma^+$	−243.0224	119.97	9c	$C_{12}Be^{2-}$	$C_{\infty v}$	$^1\Sigma^+$	−471.7800	8.27
4a	C_7Be^{2-}	$C_{\infty v}$	$^3\Sigma^-$	−281.2715	0.00	9d	$C_{12}Be^{2-}$	C_s	^{1}A	−471.7276	41.15
4b	C_7Be^{2-}	$C_{\infty v}$	$^3\Sigma^-$	−281.2650	4.10	9e	$C_{12}Be^{2-}$	C_{2v}	$^1A_1$	−471.7167	47.99
4c	C_7Be^{2-}	C_{2v}	$^1A_1$	−281.2456	16.28	9f	$C_{12}Be^{2-}$	$C_{\infty v}$	$^1\Sigma^+$	−471.6903	64.55
4d	C_7Be^{2-}	C_{2v}	$^1A_1$	−281.2333	24.00	9g	$C_{12}Be^{2-}$	$C_{\infty v}$	$^1\Sigma^+$	−471.6816	70.03
4e	C_7Be^{2-}	$C_{\infty v}$	$^3\Sigma^-$	−281.2308	25.53	9h	$C_{12}Be^{2-}$	$C_{\infty v}$	$^1\Sigma^+$	−471.6060	117.47
4f	C_7Be^{2-}	C_2	^{1}A	−281.2132	36.60	10a	$C_{13}Be^{2-}$	$C_{\infty v}$	$^3\Sigma^-$	−509.8566	0.00
4g	C_7Be^{2-}	C_{2v}	$^1A_1$	−281.2000	44.85	10b	$C_{13}Be^{2-}$	$C_{\infty v}$	$^3\Sigma^-$	−509.8541	1.57
4h	C_7Be^{2-}	$C_{\infty v}$	$^3\Sigma^-$	−281.1914	50.27	10c	$C_{13}Be^{2-}$	$C_{\infty v}$	$^3\Sigma^-$	−509.8492	4.65
4i	C_7Be^{2-}	C_{2v}	$^3B_1$	−281.1314	87.91	10d	$C_{13}Be^{2-}$	$C_{\infty v}$	$^3\Sigma^-$	−509.8461	6.63
5a	C_8Be^{2-}	$D_{\infty h}$	$^1\Sigma_g$	−319.4166	0.00	10e	$C_{13}Be^{2-}$	C_{2v}	$^1A_1$	−509.8441	7.89
5b	C_8Be^{2-}	$C_{\infty v}$	$^1\Sigma^+$	−319.4087	4.97	10f	$C_{13}Be^{2-}$	$C_{\infty v}$	$^3\Sigma^-$	−509.8293	17.14
5c	C_8Be^{2-}	$C_{\infty v}$	$^1\Sigma^+$	−319.3594	35.89	10g	$C_{13}Be^{2-}$	C_s	^{1}A	−509.8292	17.24
5d	C_8Be^{2-}	C_s	^{3}A	−319.3165	62.84	10h	$C_{13}Be^{2-}$	$C_{\infty v}$	$^3\Sigma^-$	−509.8199	23.05
5e	C_8Be^{2-}	C_{2v}	$^1A_1$	−319.3083	67.97	10i	$C_{13}Be^{2-}$	$C_{\infty v}$	$^3\Sigma^-$	−509.7521	65.63
5f	C_8Be^{2-}	$C_{\infty v}$	$^1\Sigma^+$	−319.2939	77.01	11a	$C_{14}Be^{2-}$	$C_{\infty v}$	$^1\Sigma^+$	−547.9749	0.00
5g	C_8Be^{2-}	$C_{\infty v}$	$^1\Sigma^+$	−319.2234	121.25	11b	$C_{14}Be^{2-}$	$C_{\infty v}$	$^1\Sigma^+$	−547.9720	1.82
6a	C_9Be^{2-}	$C_{\infty v}$	$^3\Sigma^-$	−357.4730	0.00	11c	$C_{14}Be^{2-}$	$C_{\infty v}$	$^1\Sigma^+$	−547.9606	8.96
6b	C_9Be^{2-}	$C_{\infty v}$	$^3\Sigma^-$	−357.4712	1.14	11d	$C_{14}Be^{2-}$	C_{2v}	$^1A_1$	−547.9259	30.73
6c	C_9Be^{2-}	$C_{\infty v}$	$^3\Sigma^-$	−357.4588	8.92	11e	$C_{14}Be^{2-}$	C_s	^{1}A	−547.9096	40.93
6d	C_9Be^{2-}	C_s	^{1}A	−357.4397	20.91	11f	$C_{14}Be^{2-}$	$D_{\infty h}$	$^1\Sigma_g$	−547.8788	60.29
6e	C_9Be^{2-}	C_{2v}	$^1A_1$	−357.4377	22.18	11g	$C_{14}Be^{2-}$	$C_{\infty v}$	$^1\Sigma^+$	−547.8769	61.45
6f	C_9Be^{2-}	$C_{\infty v}$	$^3\Sigma^-$	−357.4328	25.24	11h	$C_{14}Be^{2-}$	$C_{\infty v}$	$^1\Sigma^+$	−547.8685	66.77
6g	C_9Be^{2-}	$C_{\infty v}$	$^3\Sigma^-$	−357.3826	56.74	11i	$C_{14}Be^{2-}$	$C_{\infty v}$	$^1\Sigma^+$	−547.7911	115.33

lowest energy, and the beryllium atom is located at the fifth position as viewed from the left. The most stable $C_{14}Be^{2-}$ structure (model 11a) is with the beryllium atom located at the seventh position. Previously, Dreuw et al. reported two minima of C_4Be^{2-} and one minimum of C_6Be^{2-}; our results of models 1a and 3a are in good agreement with theirs.[36]

Models 3e and 4i are clusters with a beryllium atom bonded to one side of a cyclic C_n ring. Models 1e, 4c, 4d, and 4g are structures with a C_3 ring connected to a carbon chain with the beryllium atom located either inside or at the end of the chain. Models 6d, 8e, and 10g are structures with a C_2Be ring connected to a carbon chain via the Be atom. Among the numerous isomers, those structures with cyclic configuration are relatively common, for example, models 2d, 3c, 4f, 5e, 6e, 7d, 8g, 9e, 10e, and 11d.

In previous theoretical investigations on hetero-carbon monoanionic clusters, a configuration with the heteroatom located at the terminus of a linear carbon chain is the most favorable. However, according to our results, the linear dianion structures with the beryllium atom located at the end of a carbon chain are not the most stable isomers; they are in fact the second most stable of C_nBe^{2-} ($n = 4-6$), and the total energy becomes higher with the rise in carbon number. With the beryllium atom located inside the chain, the linear structures with an even number of carbon atoms are lower in energy.

When isomers are similar in energy, a difference in calculation method might result in a difference in the ordering of

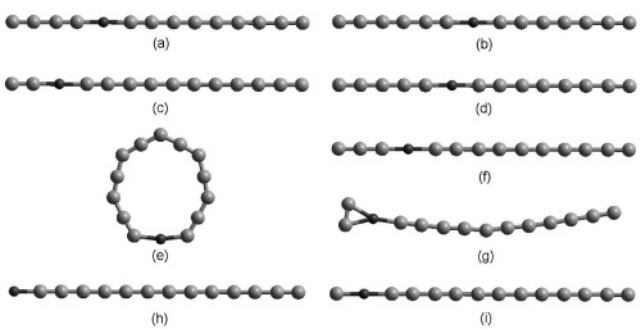

Figure 10. Nine isomers of $C_{13}Be^{2-}$.

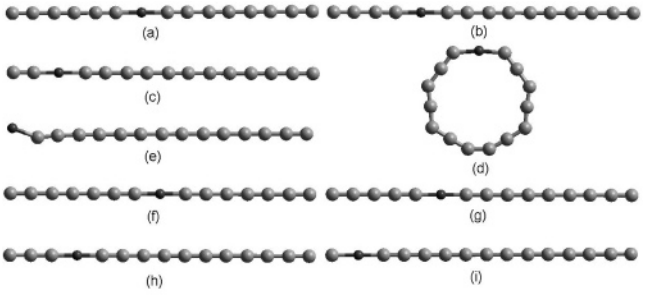

Figure 11. Nine isomers of $C_{14}Be^{2-}$.

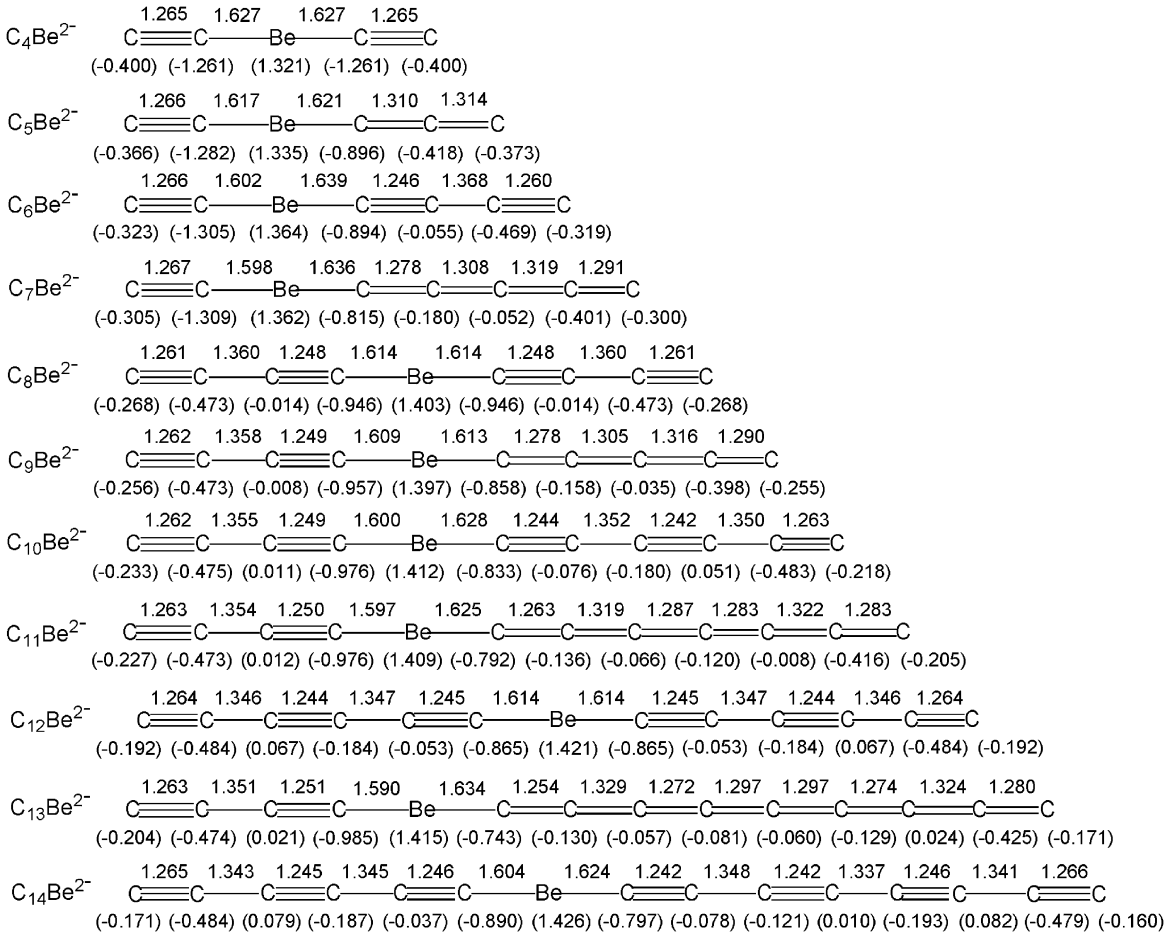

Figure 12. Bond lengths (in Å), NBO charges (in parentheses), and bond orders (number of lines between two atoms) of the most stable C_nBe^{2-} ($n = 4-14$) clusters.

energy. To test the validity of the obtained DFT energy, two different approaches, viz. CCSD(T)/6-311+G* and QCISD(T)/6-311+G* were also applied to optimize the isomers of C_4Be^{2-}. The CCSD(T) energies for 1a, 1b, 1c, 1d, 1e, 1f, and 1g are −166.5228, −166.4979, −166.4063, −166.4021, −166.3957, −166.3461, and −166.3001 au, respectively. The QCISD(T) energies are −166.5240, −166.4991, −166.4240, −166.4045, −166.3973, −166.3483, and −166.2966 au, respectively. In both cases, the ordering of energy is the same as that of B3LYP/6-311+G*. In the case of triplet state C_nBe^{2-} ($n = 4-14$) isomers, spin contamination $\langle S^2 \rangle$ value (before annihilation of the contaminants) is between 2.01 and 2.10, i.e., within 5% of the expected value of 2.0; such small deviation should not have severe effects on our results.

3.2. Bond Characters. Depicted in Figure 12 are the bond lengths, NBO charges, and bond orders of the most stable C_nBe^{2-} ($n = 4-14$) structures. The bonding of small linear carbon chains could be cumulene- or polyacetylene-like.[45] According to the results of the calculations, the lengths of the first C−C bonds as viewed from the left are within 1.261−1.267 Å, showing the characteristic of a triple bond. The C−Be and Be−C bond lengths are within 1.590−1.627 and 1.613−1.639 Å, respectively, exhibiting essentially the characteristic of a single bond. The number of carbon atoms on the left sides of the beryllium atoms are all even, and C−C bond lengths display typical short/long alternation, resembling that of polyacetylenic structures. As for the carbon chain on the right side of the beryllium atom, there is also an alternate short-and-long pattern in C−C length (1.242−1.266 and 1.337−1.368 Å) when n is even, displaying a typical polyacetylene-like character; when

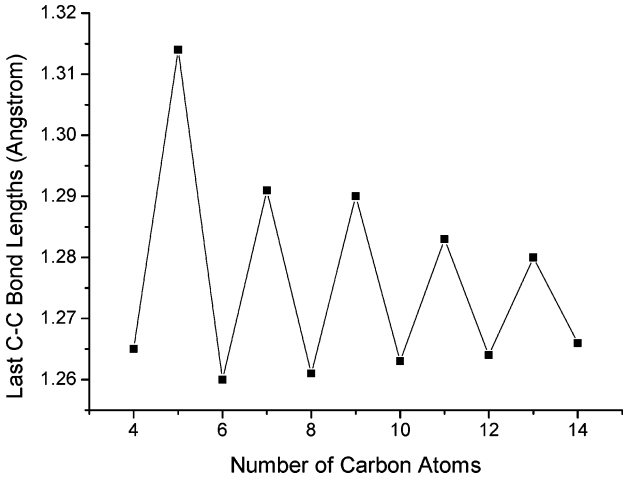

Figure 13. Length of the last C−C bond (in Å) of the most stable C_nBe^{2-} ($n = 4-14$) clusters (right side of beryllium atom as viewed in Figure 12) versus the number of carbon atoms.

n is odd, the C−C bond lengths tend to average out, exhibiting some sort of cumulenic character. As for the last C−C bonds on the right side, there is a trend of odd/even alternation: for odd n, the C−C lengths are within 1.280−1.314 Å, resembling cumulenic characters; for even n, the lengths are within 1.260−1.266 Å, corresponding to polyacetylenic characters (Figure 13). For the most stable C_nBe^{2-} ($n = 4-14$), large n-even ($n > 4$) and n-odd ($n > 5$) dianions are constructed by adding step by step a C_2 unit to small n-even and n-odd prototypes, respectively, in a strictly linear manner. For even n, the lengthened carbon

chain consists of conjugated triple and single bonds, exhibiting clear polyacetylenic character. For odd *n*, the lengthened side chain with an odd number of carbon atoms is cumulene-like in character.

Also, according to the results of NBO analysis, when *n* is even, the carbon chains on both sides of the beryllium atom are clearly characterized by a series of alternate single and triple bonds, and the dianions adopt a $(C{\equiv}C-)_xBe(-C{\equiv}C)_y$ ($x = 1-3$, $y = 1-4$) structure that shows characteristics of polyacetylene-like clusters. In other words, the two Be−C bonds are mainly single bond in character while the two terminal C−C units are triple bonds, and the linear carbon chain consists of conjugated triple and single bonds. For odd *n*, the carbon chains on the left of the beryllium atom are also characterized as polyacetylene-like whereas the carbon chains on the right-hand side are showing cumulene-like character of a whole series of double bonds.

According to the NBO charges shown in Figure 12, the majority of positive charge (in the range of 1.321−1.426) is located on the beryllium atom. There is also a sort of large/small alternation with odd/even *n*: the positive charges on the beryllium atom of even-*n* isomers are slightly larger than those of odd-*n* (except for C_4Be^{2-}), and the level of the positive charge increases with a rise in the number of carbon atoms. The negative charge is distributed among the carbon atoms, with the two carbon atoms bonded to beryllium atom showing higher levels of charging.

The structure with the heteroatom located at the end of the carbon chain is favored in energy for many hetero-carbon monoanionic clusters. As for neutral hetero-carbon clusters, Chuchev et al. studied C_nB and C_nB_2 clusters by means of the B3LYP method and found that some isomers with a boron atom at the third position are ground-state structures.[46] Klein et al. suggested two possible structures for the C_8Be^{2-} clusters; they considered the configuration of having a beryllium atom located at the end of the carbon chain (model 5c) could be more stable than the "V-shape" structure of having two side linear C_4 chains joined to the beryllium atom at an angle >100°. The reason given is that conjugation and charge separation are both greater in the former case.[31] According to our NBO charge calculation on model 5c, despite conjugation being larger in the linear structure, the beryllium atom is less able (compared to any of the carbon atoms) in stabilizing any extra charge (even as small as −0.024), and the majority of negative charge is in fact located in the carbon chain, and hence charge separation should be relatively smaller.

The strong force of Coulomb repulsion of a doubly charged anion would either enhance the emission of an electron or promote the decomposition of the molecular framework into two monoanionic fragments.[30] According to the NBO charges shown in Figure 12, the charges of beryllium atoms are positive (1.321−1.426), and dividing the conjugation system into two sections with a Be atom could obviously reduce the Coulomb repulsion force of the negative charges. The separated conjugation systems could each accommodate negative charge for better electronic stability. Hence, the interior beryllium atom plays an important role of separating the two negative charges. With the reduction in Coulomb repulsion, the dianionic structures with the beryllium atom located inside the carbon chain are more stable than those with the beryllium atom located at the end of the carbon chain.

3.3. Electronic Configuration. Shown in Table 2 are the configurations of the valence orbital of the most stable C_nBe^{2-} ($n = 4-14$) clusters. The electronic configurations are summarized as

$$(\text{core})1\sigma^2...1\pi^4...(n+2)\sigma^2\left(\frac{n}{2}\right)\pi^4 \quad n = \text{even}$$

$$(\text{core})1\sigma^2...1\pi^4...(n+2)\sigma^2\left(\frac{n+1}{2}\right)\pi^2 \quad n = \text{odd}$$

The dianionic C_nBe^{2-} ($n = 4-14$) clusters possess ($4n + 4$) valance electrons, among which are $2n$ π electrons. The outermost doubly degenerate π orbitals of linear C_nBe^{2-} clusters with even *n* are fully occupied ($^1\Sigma^+$ electronic state); for odd *n*, they are half-filled ($^3\Sigma^-$ electronic state). The HOMO with fully filled π orbitals is always energetically more stable than that with a half-filled electron shell.

The ground-state C_nBe^{2-} ($n = 4-14$) alternates between $^1\Sigma^+$ (even *n*) and $^3\Sigma^-$ (odd *n*) electron states. This arises from the fact that all MOs with π-symmetry are doubly degenerate. The addition of an extra carbon atom would result in having two more electrons included in the π-system. These electrons are accommodated in a π-orbital, resulting in a triplet state. When *n* is even, the number of alpha and beta electrons in the singlet state are equal, whereas when *n* is odd, the number of alpha electrons in the triplet state is larger (by 2) than that of the beta electrons. The effects of different parity suggest that the ground states with even *n* are more stable. The general idea is that it requires more energy to remove an electron from a closed-shell configuration (i.e., at even *n*) than from an open-shell configuration (i.e., at odd *n*).

3.4. Electron Detachment Energy and Electron Affinities. The amount of energy involved in the removal of an electron from a dianion, i.e., the electron detachment energy (EDE, adiabatic) can be obtained by computing the difference of the total energies of the optimized monoanionic and dianionic clusters (i.e., $E_{\text{monoanion}} - E_{\text{dianion}}$). When an EDE of higher value has to be applied for the removal of an electron from a dianion, the dianion is more stable with respect to electron autodetachment. Electron affinity (EA, adiabatic) is computed as the energy difference between the optimized neutral and anionic clusters (i.e., $E_{\text{neutral}} - E_{\text{monoanion}}$). A higher electron affinity would imply that more energy is released when an electron is added to the neutral molecule, and the generation of the respective monoanion is more readily done. Generally speaking, a corresponding monoanionic cluster larger in electron affinity is more stable.

Listed in Table 3 are the electron detachment energy (EDE), electron affinities (EA), atomization energy (ΔE_a), and incremental binding energy (ΔE^I) for the most stable C_nBe^{2-} ($n = 4-14$). Figure 14 depicts the EDE and EA values of the most stable C_nBe^{2-} ($n = 4-14$) dianions and the corresponding monoanions, respectively, versus the number of carbon atoms. The EDE curve of the dianions shows a pattern of mild

TABLE 2: Valence Orbital Configurations of the Most Stable C_nBe^{2-} ($n = 4-14$) Clusters

isomers	configuration
BeC_4^{2-}	(core) $\sigma^2\sigma^2\sigma^2\sigma^2\pi^4\sigma^2\sigma^2\pi^4$
BeC_5^{2-}	(core) $\sigma^2\sigma^2\sigma^2\sigma^2\sigma^2\pi^4\sigma^2\pi^4\sigma^2\pi^2$
BeC_6^{2-}	(core) $\sigma^2\sigma^2\sigma^2\sigma^2\sigma^2\sigma^2\pi^4\sigma^2\pi^4\sigma^2\pi^4$
BeC_7^{2-}	(core) $\sigma^2\sigma^2\sigma^2\sigma^2\sigma^2\sigma^2\sigma^2\pi^4\pi^4\sigma^2\pi^4\sigma^2\pi^2$
BeC_8^{2-}	(core) $\sigma^2\sigma^2\sigma^2\sigma^2\sigma^2\sigma^2\sigma^2\sigma^2\pi^4\pi^4\sigma^2\sigma^2\pi^4\pi^4$
BeC_9^{2-}	(core) $\sigma^2\sigma^2\sigma^2\sigma^2\sigma^2\sigma^2\sigma^2\sigma^2\sigma^2\pi^4\pi^4\pi^4\sigma^2\sigma^2\pi^4\pi^2$
BeC_{10}^{2-}	(core) $\sigma^2\sigma^2\sigma^2\sigma^2\sigma^2\sigma^2\sigma^2\sigma^2\sigma^2\sigma^2\pi^4\pi^4\pi^4\sigma^2\sigma^2\pi^4\pi^4$
BeC_{11}^{2-}	(core) $\sigma^2\sigma^2\sigma^2\sigma^2\sigma^2\sigma^2\sigma^2\sigma^2\sigma^2\sigma^2\sigma^2\pi^4\pi^4\pi^4\sigma^2\pi^4\sigma^2\pi^4\pi^2$
BeC_{12}^{2-}	(core) $\sigma^2\sigma^2\sigma^2\sigma^2\sigma^2\sigma^2\sigma^2\sigma^2\sigma^2\sigma^2\sigma^2\sigma^2\pi^4\pi^4\pi^4\pi^4\sigma^2\sigma^2\pi^4\pi^4$
BeC_{13}^{2-}	(core) $\sigma^2\sigma^2\sigma^2\sigma^2\sigma^2\sigma^2\sigma^2\sigma^2\sigma^2\sigma^2\sigma^2\pi^4\pi^4\pi^4\pi^4\sigma^2\pi^4\sigma^2\pi^4\pi^2$
BeC_{14}^{2-}	(core) $\sigma^2\sigma^2\sigma^2\sigma^2\sigma^2\sigma^2\sigma^2\sigma^2\sigma^2\sigma^2\sigma^2\sigma^2\sigma^2\pi^4\pi^4\pi^4\pi^4\pi^4\sigma^2\sigma^2\pi^4\pi^4$

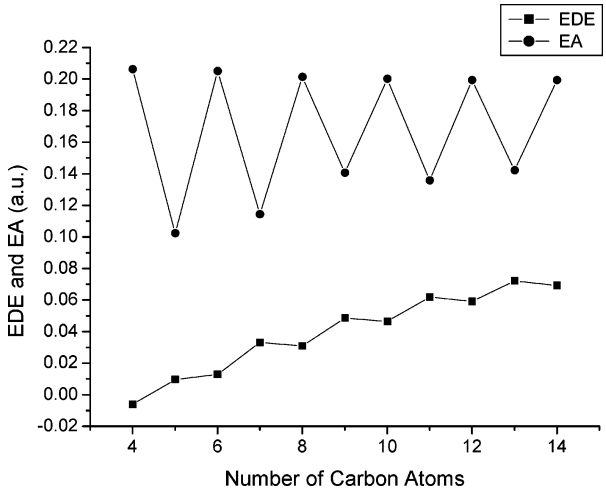

Figure 14. EDE (au) and EA (au) of the most stable C_nBe^{2-} (n = 4−14) anions and the corresponding monoanions, respectively (as shown in Table 3), versus the number of carbon atoms.

TABLE 3: Electron Detachment Energy EDE (au), Electron Affinities EA (au), Atomization Energy ΔE_a (au), and Incremental Binding Energy ΔE^I (au) of the Most Stable C_nBe^{2-} (n = 4−14)

clusters	EDE	EA	ΔE_a	ΔE^I
C_4Be^{2-}	−0.00609	0.2062	0.9025	
C_5Be^{2-}	0.0097	0.10237	1.0993	0.1968
C_6Be^{2-}	0.01291	0.20507	1.3991	0.2998
C_7Be^{2-}	0.03315	0.1144	1.5998	0.2007
C_8Be^{2-}	0.03087	0.20137	1.8877	0.2879
C_9Be^{2-}	0.04858	0.14059	2.0869	0.1992
$C_{10}Be^{2-}$	0.04649	0.20021	2.3633	0.2764
$C_{11}Be^{2-}$	0.06191	0.13577	2.5677	0.2044
$C_{12}Be^{2-}$	0.05915	0.19939	2.8355	0.2678
$C_{13}Be^{2-}$	0.07223	0.14231	3.0417	0.2063
$C_{14}Be^{2-}$	0.06926	0.19935	3.3028	0.2610

alternation, indicating that the dianions are having similar resistance against electron autodetachment. Compared to the EDE curve, the EA curve is more drastic in alternation: EA of even-*n* clusters are noticeably higher than those of odd-*n* ones. The monoanions that resulted in the fragmentation of even-*n* dianions are hence more stable than those generated in the decomposition of odd-*n* dianions. The overall results of electron detachment with due consideration to the EA and EDE values suggest that the even-*n* C_nBe^{2-} clusters are more stable than the odd-*n* C_nBe^{2-} clusters.

3.5. Incremental Binding Energies. The incremental binding energy (ΔE^I), which is the atomization energy (ΔE_a) difference of adjacent clusters, can also reflect the relative stability of the anionic clusters (Table 3).[47] It is expressed as

$$\Delta E^I = \Delta E_a(C_nBe^{2-}) - \Delta E_a(C_{n-1}Be^{2-})$$

where ΔE_a is defined as the energy difference between a molecule and its component atoms:

$$\Delta E_a = nE(C) + E(Be) - E(C_nBe^{2-})$$

As shown in Figure 15, the values of ΔE^I vary according to a pattern of odd/even alternation: When n is even, the ΔE_n value is big; when n is odd, the ΔE_n is small. Because a larger ΔE^I value implies a more stable C_nBe^{2-} structure, one can deduce that a C_nBe^{2-} cluster with even n is more stable than one with odd n. Such an odd/even alternate pattern of electron affinity and incremental binding energy is consistent with the

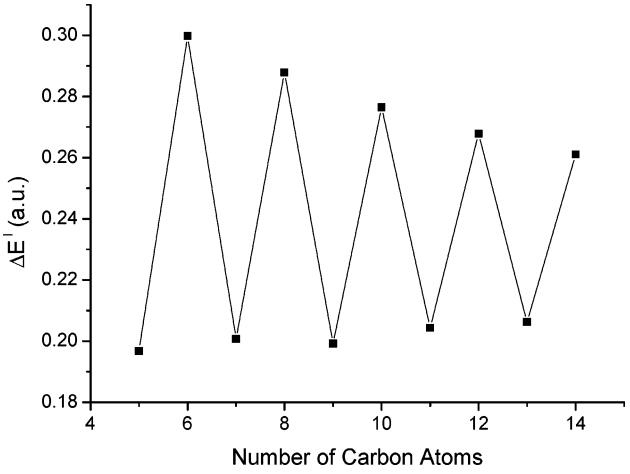

Figure 15. Incremental binding energies ΔE^I (kcal/mol) of the most stable linear C_nBe^{2-} (n = 4−14) clusters (as shown in Table 3) versus the number of carbon atoms.

experimental observation of Klein et al.[31] The missing of odd-*n* peaks or products in experimental studies can be explained by a combined consideration of the overall behaviors of electron detachment (EA and EDE) and the incremental binding energies of the dianionic clusters. Since the electron affinities of the corresponding monoanionic clusters and the incremental binding energies of the dianionic clusters are obviously low when n is odd, compared to the even-*n* clusters, the odd-*n* ones are less stable and more susceptible to fragmentation.

4. Conclusions

The ground-state structures of C_nBe^{2-} (n = 4−14) are linear with the beryllium atom located inside the C_n chain. For the side chains with an even number of carbon atoms, the bond lengths and bond orders suggest a polyacetylene-like structure, whereas for the side chains with an odd number of carbon atoms, the data suggest a cumulenic-like arrangement. The dianionic clusters with "even-*n*" are more stable than those with "odd-*n*". The trend of odd/even alternation can be explained according to the variation of bonding character, electronic configuration, electron detachment, and incremental binding energy. The results of calculation are in good agreement with the relative intensity of the C_nBe^{2-} (n = 4−14) species observed in experimental studies.

Acknowledgment. This work was supported by the National Science Foundation of China (Grants 20473061 and 20533020).

References and Notes

(1) Weltner, W., Jr.; Van Zee, R. J. *Chem. Rev.* **1989**, *89*, 1713.
(2) Raghavachari, K.; Binkley, J. S. *J. Chem. Phys.* **1987**, *87*, 2191.
(3) Consalvo, D.; Mele, A.; Stranges, D.; Giardini-Guidoni, A.; Teghil, R. *Int. J. Mass Spectrom. Ion Processes* **1989**, 91, 319.
(4) Leleyter, M.; Joyes, P. *Surf. Sci.* **1985**, *156*, 800.
(5) Orth, R. G.; Jonkmann, H. T.; Michl, J. *Int. J. Mass Spectrosc. Ion Processes* **1982**, *43*, 41.
(6) Becker, S.; Dietze, H. J. *Int. J. Mass Spectrosc. Ion Processes* **1988**, *82*, 287.
(7) Huang, R. B.; Wang, C. R.; Liu, Z. Y.; Zheng, L. S.; Qi, F.; Sheng, L. S.; Yu, S. Q.; Zhang, Y. W. *Z. Phys. D* **1995**, *33*, 49.
(8) Wang, H. Y.; Huang, R. B.; Chen, H.; Lin, M. H.; Zheng, L. S. *J. Phys. Chem. A* **2001**, *105*, 4653.
(9) Zhan, C. G.; Iwata, S. *J. Chem. Phys.* **1996**, *104*, 9058.
(10) Pascoli, G.; Lavendy, H. *Chem. Phys. Lett.* **1999**, *312*, 333.
(11) Zhan, C. G.; Iwata, S. *J. Phys. Chem. A* **1997**, *107*, 591.
(12) Zhan, C. G.; Iwata, S. *J. Chem. Phys.* **1997**, *107*, 7323.
(13) Pascoli, G.; Lavendy, H. *J. Phys. Chem. A* **1999**, *103*, 3518.
(14) Fisher, K.; Dance, I.; Willett, G. *Eur. Mass Spectrom.* **1997**, *3* (5), 331.

(15) Li, G. L.; Tang, Z. C. *J. Phys. Chem. A* **2003**, *107*, 5317.
(16) Hunsicker, S.; Jones, R. O. *J. Chem. Phys.* **1996**, *105*, 5048.
(17) Gomei, M.; Kishi, r.; Nakajima, A.; Iwata, S.; Kaya, K. *J. Chem. Phys.* **1996**, *107*, 10051.
(18) Wang, H. Y.; Huang, R. B.; Chen, H.; Lin, M. H.; Zheng, L. S. *J. Phys. Chem. A* **2001**, *105*, 4653.
(19) Vandenbosch, R.; Will, D. I. *J. Chem. Phys.* **1996**, *104*, 5600.
(20) Pan, L.; Rao, B. K.; Gupta, A. K.; Das, G. P.; Ayyub, P. *J. Chem. Phys.* **2003**, *119*, 7705.
(21) Li, G. L.; Xing, X. P.; Tang, Z. C. *J. Chem. Phys.* **2003**, *118*, 6884.
(22) Redondo, P.; Barrientos, C.; Cimas, A.; Largo, A. *J. Phys. Chem. A* **2003**, *107*, 4676.
(23) Redondo, P.; Barrientos, C.; Cimas, A.; Largo, A. *J. Phys. Chem. A* **2003**, *107*, 6312.
(24) Largo, A.; Redondo, P.; Barrientos, C. *J. Phys. Chem. A* **2004**, *108*, 6421.
(25) Redondo, P.; Barrientos, C.; Cimas, A.; Largo, A. *J. Phys. Chem. A* **2004**, *108*, 212.
(26) Largo, A.; Redondo, P.; Barrientos, C. *J. Phys. Chem. A* **2002**, *106*, 4217.
(27) Redondo, P.; Barrientos, C.; Largo, A. *Int. J. Quantum Chem.* **2004**, *96*, 615.
(28) Largo, A.; Cimas, A.; Redondo, P.; Barrientos, C.; *Int. J. Quantum Chem.* **2001**, *84*, 127.
(29) Liu, J. W.; Chen, M. D.; Zheng, L. S.; Zhang, Q. E.; Au, C. T. *J. Phys. Chem. A* **2004**, *108*, 5704.
(30) Dreuw, A.; Cederbaum, L. S. *Chem. Rev.* **2002**, *102*, 181.
(31) Klein, J.; Middleton, R. *Nucl. Instrum. Methods Phys. Res. B* **1999**, *159*, 8.
(32) Gnaser, H. *Phys. Rev. A* **1999**, *60*, R2645.
(33) Gnaser, H.; Dreuw, A.; Cederbaum, L. S. *J. Chem. Phys.* **2002**, *117*, 7002.
(34) Dreuw, A.; Sommerfeld, T.; Cederbaum, L. S. *J. Chem. Phys.* **1998**, *109*, 2727.
(35) Dreuw, A.; Sommerfeld, T.; Cederbaum, L. S. *Angew. Chem., Int. Ed. Engl.* **1997**, *36*, 1889.
(36) Dreuw, A.; Cederbaum, L. S. *J. Chem. Phys.* **2000**, *112*, 7400.
(37) Shi, Q. C.; Kais, S. *J. Am. Chem. Soc.* **2002**, *124*, 11723.
(38) Trindle, C.; Yumak, A. *J. Chem. Theory Comput.* **2005**, *1*, 1038
(39) *Hyerchem Reference Manual*; Hypercube Inc.: Waterloo, Ontario, Canada, 1996.
(40) Frisch, M. J.; Trucks, G. W.; Schlegel, H. B.; Scuseria, G. E.; Robb, M. A.; Cheeseman, J. R.; Zakrzewski, V. G.; Montgomery, J. A.; Stratmann, Jr., R. E.; Burant, J. C.; Dapprich, S.; Millam, J. M.; Daniels, A. D.; Kudin, K. N.; Strain, M. C.; Farkas, O.; Tomasi, J.; Barone, V.; Cossi, M.; Cammi, R.; Mennucci, B.; Pomelli, C.; Adamo, C.; Clifford, S.; Ochterski, J.; Petersson, G. A.; Ayala, P. Y.; Cui, Q.; Morokuma, K.; Malick, D. K.; Rabuck, A. D.; Raghavachari, K.; Foresman, J. B.; Cioslowski, J.; Ortiz, J. V.; Baboul, A. G.; Stefanov, B. B.; Liu, G.; Liashenko, A.; Piskorz, P.; Komaromi, I.; Gomperts, R.; Martin, R. L.; Fox, D. J.; Keith, T.; Al-Laham, M. A.; Peng, C. Y.; Nanayakkara, A.; Gonzalez, C.; Challacombe, M.; Gill, P. M. W.; Johnson, B.; Chen, W.; Wong, M. W.; Andres, J. L.; Gonzalez, C.; Head-Gordon, M.; Replogle, E. S.; Pople, J. A. *Gaussian 98 (Revision A.7)*; Gaussian, Inc.: Pittsburgh, PA, 1998.
(41) Beche, A. D. *J. Chem. Phys.* **1993**, *98*, 5648.
(42) Lee, C.; Yang, W.; Parr, R. G. *Phys. Rev. B* **1988**, *37*, 785.
(43) Hehre, W. J.; Radom, L.; Schleyer, P. V. R.; Pople, J. A. *Ab Initio Molecular Orbital Theory*; Wiley-Interscience: New York, 1986.
(44) Foresman J. B.; Frisch, AE. *Exploring Chemistry with Electronic Structure Methods*; Gaussian: Pittsburgh, PA, 1996.
(45) Parent, D. C.; Anderson, S. L. *Chem. Rev.* **1992**, *92*, 1541.
(46) Chuchev, K.; BelBruno, J. J. *J. Phys. Chem. A* **2004**, *108*, 5226.
(47) Pascoli, G.; Lavendy, H. *Int. J. Mass Spectrom. Ion Processes* **1998**, *173*, 41.